

# Mass Spectrometric and Theoretical Study of Polyiodides: The Connection between Solid State, Solution, and Gas Phases

Michael Groessl,<sup>†,||</sup> Zhaofu Fei,<sup>†</sup> Paul J. Dyson,<sup>\*,†</sup> Sergey A. Katsyuba,<sup>\*,‡</sup> Krista L. Vikse,<sup>§</sup> and J. Scott McIndoe<sup>\*,§</sup>

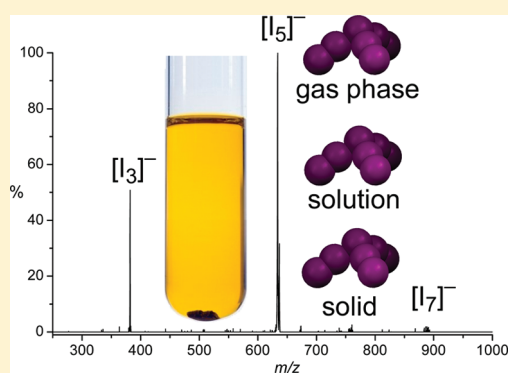
<sup>†</sup>Institut des Sciences et Ingénierie Chimiques, Ecole Polytechnique Fédérale de Lausanne (EPFL), CH-1015 Lausanne, Switzerland

<sup>‡</sup>A. E. Arбузов Institute of Organic and Physical Chemistry, Kazan Scientific Center of Russian Academy of Sciences, Arbuzov str., 8, 420088, Kazan, Russia

<sup>§</sup>Department of Chemistry, University of Victoria, P.O. Box 3065, Victoria, BC V8W 3 V6, Canada

 Supporting Information

**ABSTRACT:** Polyiodides have been transferred intact from acetonitrile solution to the gas phase and analyzed by mass spectrometry. A range of ions were observed, including  $[I_{11}]^-$ ,  $[I_{13}]^-$ , and  $[I_{15}]^-$ , which have higher iodine/iodide ratios than any previously characterized ions. Theoretical calculations show that branched structures are strongly favored, a result which is in excellent agreement with gas phase fragmentation studies (MS/MS) and also previous solid state studies. This study demonstrates the utility of mass spectrometry to provide structural information in the absence of other spectroscopic handles.



## INTRODUCTION

Polyiodide salts are a structurally diverse and highly complex class of compounds.<sup>1</sup> Their extraordinary properties, especially those related to their conductivity, have led to widespread applications in electronics,<sup>2</sup> batteries,<sup>3</sup> optical devices,<sup>4</sup> and dye-sensitized solar cells.<sup>5</sup> Despite their complexity, polyiodides are simple to make by mixing elemental iodine with iodide salts in appropriate ratios.<sup>6</sup> The structure of the polyiodide depends on both the  $I_2/I^-$  ratio and the counteraction,<sup>7</sup> and in the solid state large cations and/or those with multiple charge result in the largest and most structurally diverse polyiodide anions. Structures often contain multiple polyiodides, a classic case being  $[Lu(\text{dibenzo-18-crown-6})(H_2O)_3(\text{thf})_6]^{3+}$ , which crystallizes with 2 equiv of  $[I_3]^-$ , 6 of  $[I_5]^-$ , and 1 each of  $[I_8]^{2-}$  and  $[I_{12}]^{2-}$ .<sup>8</sup> The most iodine-rich polyiodide corresponds to the ferrocenium salt of  $[I_{29}]^{3-}$ ,<sup>9</sup> which comprises a three-dimensional (3D) network made up of  $[I_5]^-$ ,  $[I_{12}]^{2-}$ , and  $I_2$  units. Polyiodides can alternatively be thought of as comprising  $I_2$  and  $I^-$  and/or  $[I_3]^-$  units linked through donor–acceptor interactions.<sup>10</sup>

Despite the manifest richness of the solid-state structures of polyiodides, much less is known about their existence in solution or in the gas phase. Polyiodides in solution are dominated by  $[I_3]^-$ , but contain a complex mixture of higher polyiodides in low concentration, and lacking a diagnostic spectroscopic handle, they are not easily studied. It has even been stated that there is *no*

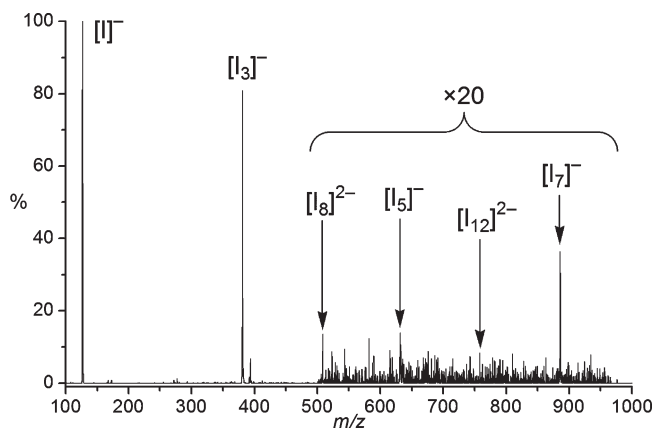
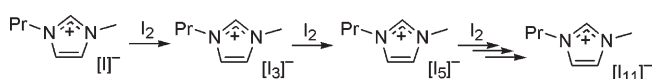
experimental evidence for the formation of higher polyiodides in aqueous solution.<sup>11</sup> Electrospray ionization mass spectrometry (ESI-MS)<sup>12</sup> is a technique capable of analyzing solution speciation in detail,<sup>13</sup> including very labile species (provided conditions are carefully selected).<sup>14</sup> Consequently, polyiodides are ideal analytes for the technique, as most of the likely species differ in  $m/z$  and ESI-MS is well-suited to the study of complex mixtures (fragmentation is minimal and all separation is carried out in the gas phase). Consistent with other spectroscopic techniques, previous studies of polyiodides by ESI-MS have not detected any iodides higher than  $[I_3]^-$  regardless of the overall composition,<sup>15</sup> although ESI-MS was not the principal focus of these investigations. We set out with the higher polyiodides as our principal focus, and based on the importance of polyiodides in solar cells, selected the benchmark system 1-propyl-3-methylimidazolium (pmim) iodide/iodine,<sup>16</sup> and remarkably, excellent correlations between these gas phase studies and previous studies on polyiodides in the solid state were obtained.

## RESULTS AND DISCUSSION

A series of polyiodide ionic liquids  $[pmim][I] \cdot nI_2$  ( $n = 1-5$ ) were prepared by addition of the appropriate amount of iodine to  $[pmim][I]$  (Scheme 1), diluted in acetonitrile and analyzed by

Received: July 29, 2011

Published: September 01, 2011

**Scheme 1. Preparation of Polyiodides under Solvent-Free Conditions**


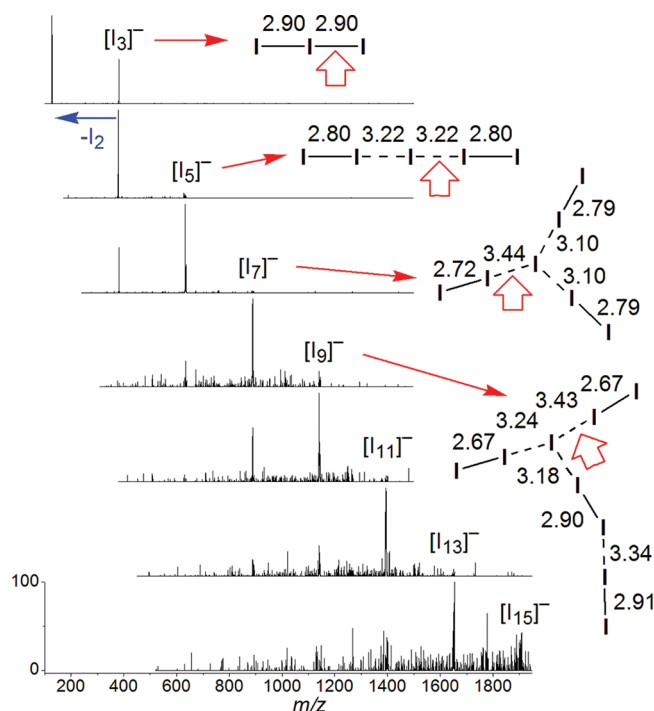
**Figure 1.** Negative-ion ESI-MS of  $[\text{pmim}][\text{I}]\cdot 4\text{I}_2$  ( $10\ \mu\text{mol L}^{-1}$ ) in acetonitrile. The spectral region above  $m/z$  500 is shown at an intensity  $20\times$  that recorded, to reveal the higher polyiodides.

ESI-MS (see Experimental Section). Solutions of  $10\ \mu\text{M}$  based on iodide were used since it was found that at higher concentrations the spectra were complicated by the appearance of aggregates containing the cation,<sup>17</sup> namely,  $[(\text{pmim})_n(\text{I}_3)_{(n+1)}]^-$ ,  $[(\text{pmim})_n(\text{I})_{(n+1)}]^-$ , and combinations of the two. The solutions were stable; speciation did not change over several days of analysis, and no special precautions were taken.

At first glance the negative-ion ESI-MS of  $[\text{pmim}][\text{I}]\cdot 4\text{I}_2$  appears to contain only  $[\text{I}]^-$  and  $[\text{I}_3]^-$ . The higher polyiodides are present in very low abundance as the spectra are recorded near the sensitivity limit of the instrument to avoid the appearance of aggregate ions (see above). Nonetheless, close inspection at higher  $m/z$  reveals a variety of characteristically monoisotopic ions (Figure 1).

The  $m/z$  value gives a good indication of the likely identity of each ion with unambiguous confirmation provided by tandem MS. The anions  $[\text{X}_3]^-$  ( $\text{X} = \text{Cl}, \text{Br}, \text{I}$ ) fragment predominantly by loss of  $\text{X}_2$ , although via a minor fragmentation mechanism  $\text{X}\cdot$  can also be lost to leave a detectable radical anion.<sup>18</sup> All of the polyiodides  $[\text{I}_{2n+1}]^-$  ( $n = 1-7$ ) were found to fragment by  $\text{I}_2$  loss (Figure 2) through collision-induced dissociation (CID) in the ion trap, and in each case the base peak in the MS/MS is  $[\text{I}_{2n-1}]^-$ .

There are different pathways by which the fragmentation of the monoanionic polyiodides  $[\text{I}_{2n+1}]^-$  ( $n = 1-7$ ) might proceed. In principle, cleavage may occur at any bond, although most likely where two even-electron fragments are generated rather than two radicals. Such bonds are found to be longest in the solid-state structures. For example, assuming  $[\text{I}_{15}]^-$  has a linear structure, fragmentation might be expected to occur with equal efficiency at any point in the chain and the fragments  $[\text{I}_{2n+1}]^-$  ( $n = 1-7$ ) would appear with roughly the same abundance. However, such a pattern is not observed, and instead, the dominant fragmentation involves loss of iodine. This observation is consistent not only with the polyiodides observed in solid state



**Figure 2.** Negative-ion ESI-MS/MS of the ions  $[\text{I}_{2n+1}]^-$  ( $n = 1-7$ ). The precursor ion in each case is labeled. Fragmentation proceeds through sequential loss of  $\text{I}_2$ . The base product ion peak in all MS/MS spectra is the loss of one  $\text{I}_2$ , but loss of two and even three  $\text{I}_2$  units can be observed. To the right of the spectra, crystallographically determined connectivity and bond lengths ( $\text{\AA}$ ) for  $[\text{I}_9]^-$ ,  $[\text{I}_7]^-$ ,  $[\text{I}_5]^-$ , and  $[\text{I}_3]^-$  are shown.<sup>1</sup> Note that breaking the longest bond leads to  $\text{I}_2$  loss in all cases, consistent with the MS/MS results.

**Table 1. Calculated Bond Lengths ( $r/\text{\AA}$ ) and Vibrational Frequencies ( $\nu/\text{cm}^{-1}$ ) of  $\text{I}_2$ ,  $\text{I}_2^-$ ,  $\text{I}_3^-$ , and  $\text{I}_5^-$  from This Work and Selected Literature Values**

ion	method	r1	r2	$\nu_1$	$\nu_2$	$\nu_3$
$\text{I}_2$	CCSD(T)/ECP-TZ(2df) <sup>a</sup>	2.709		210.2		
$\text{I}_2$	B3LYP/SC-ECP <sup>b</sup>	2.703		213.2		
$[\text{I}_2]^-$	CCSD(T)/ECP-TZ(2df) <sup>a</sup>	3.299		105.5		
$[\text{I}_2]^-$	B3LYP/SC-ECP <sup>b</sup>	3.331		89.5		
$[\text{I}_3]^-$	CCSD(T)/ECP-TZ(2df) <sup>a</sup>	2.982		107.8	58.2	129.3
$[\text{I}_3]^-$	B3LYP/SC-ECP <sup>b</sup>	2.994		105.3	53.8	133.2
$[\text{I}_5]^-$	B3PW91/ECP-TZ(2df) <sup>a</sup>	2.857	3.065	157.4 <sup>c</sup>	143.5 <sup>c</sup>	109.9 <sup>c</sup>
$[\text{I}_5]^-$	B3LYP/SC-ECP <sup>b</sup>	2.884	3.103	152.5 <sup>c</sup>	138.7 <sup>c</sup>	96.6 <sup>c</sup>

<sup>a</sup> Ref 20a. <sup>b</sup> This work. <sup>c</sup>  $\nu_1$ ,  $\nu_2$ ,  $\nu_3$  here correspond to  $\omega_9$ ,  $\omega_8$ , and  $\omega_7$ , respectively, in ref 20a.

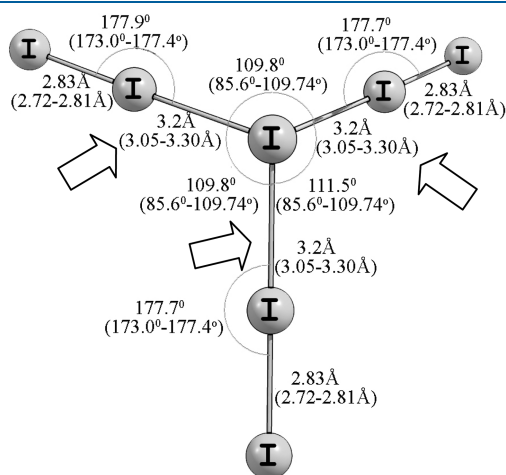
structures,<sup>1</sup> but also with a theoretical study on the solid-state polybromides  $[\text{Br}_{2n+1}]^-$  ( $n = 1-4$ ) which found that the most stable structures are those that are heavily branched.<sup>19</sup> The MS/MS data suggests that branched structures are also likely for these higher polyiodides.

Because no crystallographic data is available for the anions  $[\text{I}_{11}]^-$ ,  $[\text{I}_{13}]^-$ , or  $[\text{I}_{15}]^-$ , and only  $[\text{I}_2]^-$ ,  $[\text{I}_3]^-$ , and  $[\text{I}_5]^-$  gas-phase structures of polyiodides have been studied quantum-chemically, we addressed this limitation and performed calculations on all of the species observed by ESI-MS.<sup>20</sup> Computations for these systems, as well as for the benchmark  $\text{I}_2$ , are in reasonable

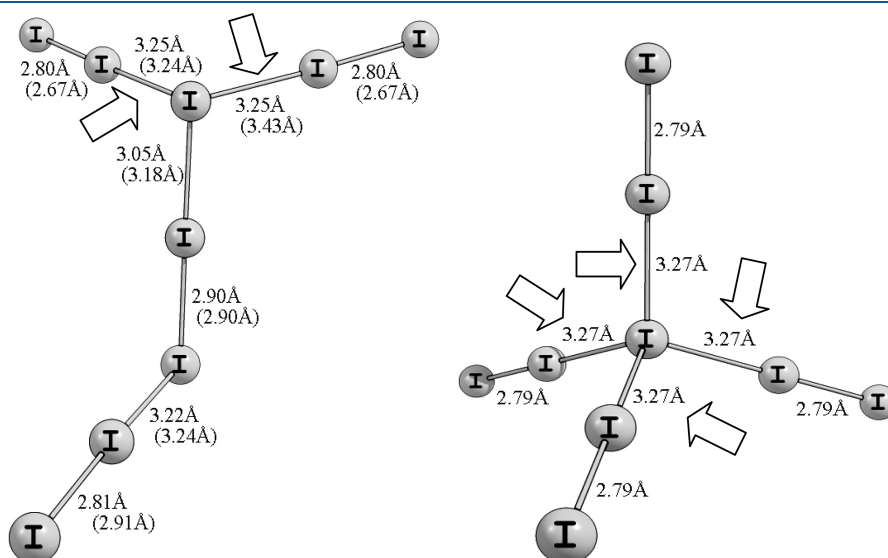
agreement with the previously published theoretical studies (Table 1).

For larger  $[I_{(2n+1)}]^-$  anions ( $n = 3, 4$ ), as well as for  $[I_{2n}]^{2-}$  ( $n = 4$ ) dianions, neither quantum-chemical nor experimental gas phase data are available, so the optimized geometry parameters of the hepta-, octa-, and nona-iodides were compared with the corresponding crystallographic data (Figures 3–5, respectively). Reasonable agreement of the computations for the isolated anions with the experimental data obtained for the solids suggests that the influence of the counterions and lattice surrounding the structure of the polyiodides is not crucial, with the anions adopting similar topologies in the gas, solution, and solid phases.

Attempts were made to find stable forms of the polyiodides that have not been characterized in crystals. These computations, indeed, revealed a “tetrahedral” structure for  $[I_9]^-$  (Figure 4),



**Figure 3.** Optimized structure of  $[I_7]^-$ . The computed geometry parameters are given with the corresponding crystallographically determined values (in parentheses) from ref 1. Arrows indicate the longest bonds.

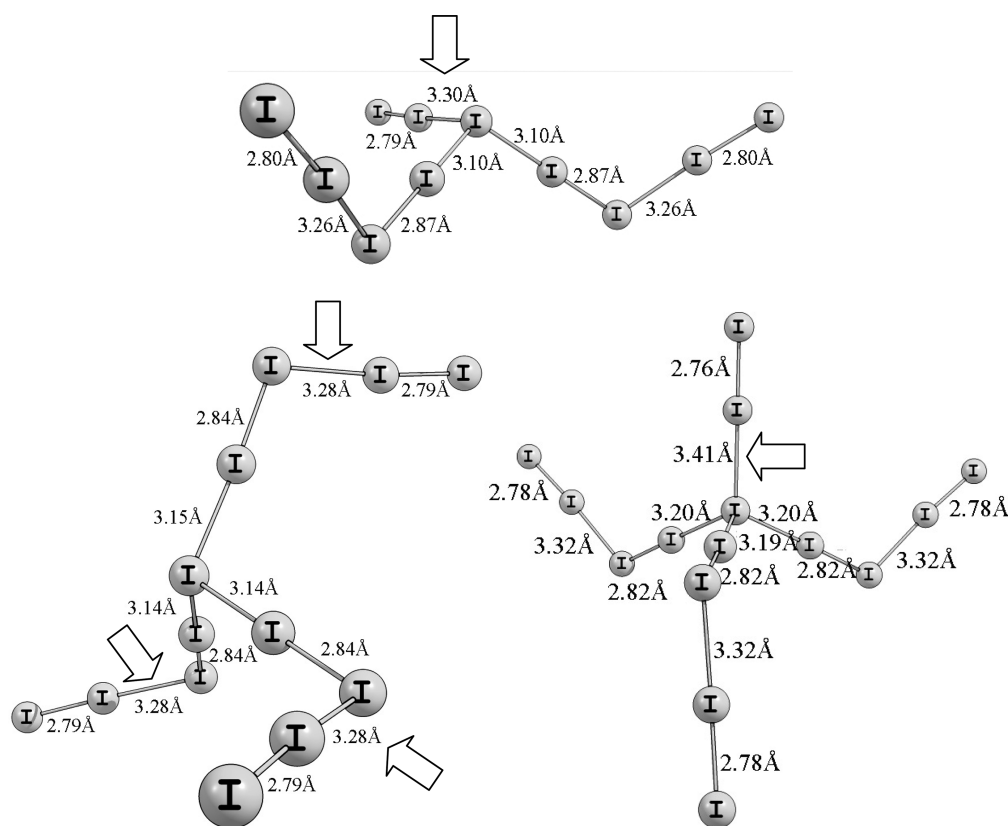


**Figure 4.** Optimized structure of  $[I_9]^-$  (left) with the computed bond lengths and the corresponding crystallographically determined values (in parentheses) from ref 1.  $E = -2662.5367015$  au ( $-1670741.8$  kcal/mol); sum of electronic and zero-point energies =  $-2662.533522$  a.u ( $-1670739.8$  kcal/mol). Optimized “tetrahedral” structure of  $[I_9]^-$  (right) and the computed bond lengths.  $E = -2662.533585$  au ( $-1670739.8$  kcal/mol); sum of electronic and zero-point energies =  $-2662.530574$  au ( $-1670737.9$  kcal/mol) Arrows indicate the longest bonds.

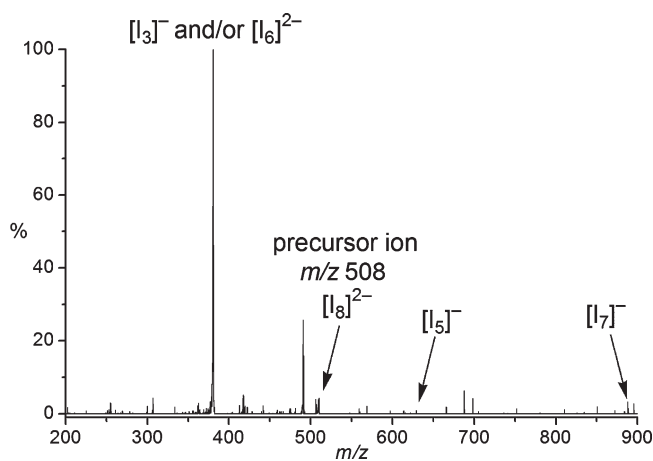
being more heavily branched than typical “pyramidal” structure shown in Figure 3, the former being less energetically stable than the latter by about  $2$  kcal·mol $^{-1}$ . The more stable “pyramidal”  $[I_9]^-$  configuration was used as a basis to build up hypothetical, arbitrary structures of undeca-iodide  $[I_{11}]^-$ , trideca-iodide  $[I_{13}]^-$ , and pentadeca-iodide  $[I_{15}]^-$ . Optimization of these starting geometries resulted in the stable structures shown in Figure 5.

In all cases, the longest bonds in the computationally determined structures involve a bond to a terminal  $I_2$  moiety, and breaking this fragment would give rise to a loss of  $-254$  Da as the primary fragmentation process in the MS/MS investigations, which is in fact what is observed. In principle, doubly charged polyiodides could also be fragmented by  $I_2$  loss, and might also cleave in an asymmetrical fashion, to produce two monoanionic (poly)iodides (homolytic cleavage seems less likely, as two radical anions would be obtained). The only two dianionic polyiodides observed in the ESI-MS that do not overlap with monoanions are  $[I_8]^{2-}$  and  $[I_{12}]^{2-}$ , both of which have been characterized in the solid state.<sup>8</sup> We have assigned these as dianions rather than the monoanions  $[I_4]^-$  and  $[I_6]^-$ , simply because the monoanions would not be even-electron species.  $[I_8]^{2-}$  provided an MS/MS dominated by a product ion at  $m/z$  381, which could correspond to  $[I_3]^-$ ,  $[I_6]^{2-}$ , or quite likely, both (Figure 6).  $[I_6]^{2-}$  has a high charge density, and as polyanions have a limited lifetime in the gas phase, it is likely to separate into  $2 \times [I_3]^-$  in the gas phase, an example of an ion fragmenting into a product ion with the same  $m/z$  ratio. The two ions are indistinguishable as iodine is monoisotopic.  $[I_{12}]^{2-}$  exhibited analogous behavior to  $[I_8]^{2-}$ , and there is evidence for  $[I_8]^{2-}$  and  $[I_{12}]^{2-}$  as product ions in the spectra of  $[I_5]^-$  and  $[I_7]^-$  (see Supporting Information), suggested that there is some  $[I_{10}]^{2-}$  and  $[I_{14}]^{2-}$  present in solution.

No stable forms were found computationally for  $[I_8]^{2-}$ , instead the linear form seen in Figure 7 was found to be stable. These results are in agreement with the observation that though a lot of branched forms of  $[I_{(2n+1)}]^-$  anions are present in crystals,<sup>1</sup> whereas only one branched structure of  $[I_8]^{2-}$ , with an

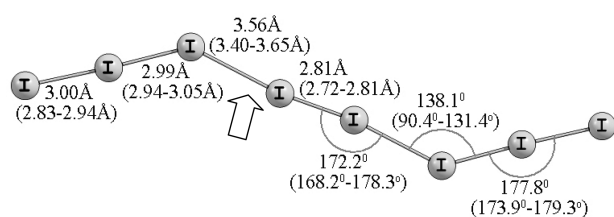


**Figure 5.** Optimized structures and the computed bond lengths of [I<sub>11</sub>]<sup>-</sup> ( $E = -3254.179579$  au =  $-2041997.7$  kcal/mol); sum of electronic and zero-point energies =  $-3254.175643$  au =  $-2041995.2$  kcal/mol); [I<sub>13</sub>]<sup>-</sup> ( $E = -3845.820434$  au =  $-2413252.3$  kcal/mol); sum of electronic and zero-point energies =  $-3845.815815$  au =  $-24113249.4$  kcal/mol); [I<sub>15</sub>]<sup>-</sup> ( $E = -4437.457103$  au =  $-2784504.3$  kcal/mol); sum of electronic and zero-point energies =  $-4437.451642$  au =  $-2784504.3$  kcal/mol)). Arrows indicate the longest bonds.



**Figure 6.** ESI-MS/MS of [I<sub>8</sub>]<sup>2-</sup>. The identity of the peak at  $m/z$  490 is unknown, but is likely to be a fragment from an ion coincident with the precursor ion at  $m/z$  508. The loss of 18 Da is consistent with elimination of water, a common fragmentation pathway for polar molecules, and confirms that the ion is not related to the polyiodide species.

unusual [(I<sub>5</sub><sup>-</sup>) · (I<sub>3</sub><sup>-</sup>)] configuration, has been reported.<sup>21</sup> Moreover, the linear structure is consistent with the MS/MS study, as cleavage of the longest bond (3.56 Å) would produce [I<sub>5</sub>]<sup>-</sup> and [I<sub>3</sub>]<sup>-</sup>. The low abundance of [I<sub>5</sub>]<sup>-</sup> suggests that it is prone to



**Figure 7.** Optimized structure of [I<sub>8</sub>]<sup>2-</sup>. The computed geometry parameters and the corresponding crystallographic data (in parentheses) taken from ref 1. The arrow indicates the longest bond.

further fragmentation via I<sub>2</sub> loss, and the appearance of [I<sub>7</sub>]<sup>-</sup> suggests that a small amount of the precursor ion fragments via the pathway [I<sub>8</sub>]<sup>2-</sup> → [I<sub>7</sub>]<sup>-</sup> + [I]<sup>-</sup>.

In summary, a large number of polyiodides including [I<sub>2n+1</sub>]<sup>-</sup> ( $n = 1-7$ ) and [I<sub>2n</sub>]<sup>2-</sup> ( $n = 4-7$ ) were transferred to the gas phase and identified by ESI-MS(/MS). [I<sub>11</sub>]<sup>-</sup>, [I<sub>13</sub>]<sup>-</sup>, and [I<sub>15</sub>]<sup>-</sup> have higher iodine/iodide ratios than any previously characterized polyiodide. These species are present in solution, and it is likely that their abundance increases with concentration (as the solubility of free iodine decreases). Indeed, many of the polyiodides observed by MS have been observed in the solid state, which suggests that the exotic solid state structures characterized by crystallography may have their components prefabricated in solution. Stable structures were calculated for all [I<sub>2n+1</sub>]<sup>-</sup> ions, and branched structures with the longest bond lengths to terminal



I<sub>2</sub> units were predicted, hence confirming the observed fragmentation pattern in the MS/MS experiments. This study demonstrates the utility of ESI-MS(/MS) in the discovery of new polyiodides, and has shown that correlations between gas, solution, and solid phases are justified.

## EXPERIMENTAL SECTION

The polyiodide salt [pmim][I]·4I<sub>2</sub>, where [pmim] = the 1-propyl-3-methyl-imidazolium cation, was prepared by addition of 4 equiv of elemental iodine to the 1-propyl-3-methylimidazolium iodide salt at room temperature. For mass spectrometric analysis, a 10 μmol L<sup>-1</sup> solution in acetonitrile (HPLC grade, Acros) was prepared. Mass spectra were collected in negative ion mode on a ThermoFinnigan LCQ DecaXP Plus quadrupole ion trap instrument (Thermo Fisher Scientific, Bremen, Germany) equipped with an orthogonal ESI ion source in the range from *m/z* 100–2000. Samples were infused directly into the source at a flow rate of 5 μL min<sup>-1</sup> using a syringe pump. The spray voltage was set at 4 kV, the capillary temperature at 100 °C and the capillary voltage at -6 V. For CID experiments, an isolation width of 10 Da and a relative collision energy of 25% were used. Data acquisition and analysis were carried out using the Xcalibur software package (Thermo Fisher Scientific).

All quantum-chemical calculations were carried out using the Gaussian-03 suite of programs.<sup>22</sup> Becke's three-parameter exchange functional<sup>23</sup> was used in combination with the Lee–Yang–Parr correlation functional (B3LYP).<sup>24</sup> Following full geometry optimizations without any symmetry constraints, all stationary points were characterized as minima by analysis of the Hessian matrices. Calculations were carried out with the aug-cc-pVTZ basis set including small-core energy consistent relativistic pseudopotentials (MDF-28 SC-ECPs)<sup>25</sup> from the Stuttgart and Dresden (SDD) basis set library.<sup>26</sup>

## ASSOCIATED CONTENT

**S Supporting Information.** Further details are given in Figures SII–SI8. This material is available free of charge via the Internet at <http://pubs.acs.org>.

## AUTHOR INFORMATION

### Corresponding Authors

\*E-mail: paul.dyson@epfl.ch (P.J.D.); skatsyuba@yahoo.com (S.A.K.); mcindoe@uvic.ca (J.S.M.).

### Present Addresses

<sup>||</sup>Max Planck Institute of Molecular Cell Biology and Genetics, 01307 Dresden, Germany.

## ACKNOWLEDGMENT

S.A.K. thanks Dr. G. Shamov for valuable advice on quantum-chemical computations. The EPFL and Swiss National Science Foundation (P.J.D.) and the Austrian Science Foundation (Schrödinger Fellowship J2882-N19 to M.G.) are thanked for financial support. J.S.M. thanks NSERC (Discovery and Discovery Accelerator Supplement), CFI and BCKDF for operational and infrastructure funding. K.L.V. thanks the University of Victoria for a Pacific Century fellowship.

## REFERENCES

(1) Svensson, P. H.; Kloo, L. *Chem. Rev.* **2003**, *103*, 1649.  
(2) Owens, B. B.; Patel, B. K.; Skarstad, P. M.; Warburton, D. L. *Solid State Ionics* **1983**, *9–10*, 1241.

(3) Licht, S.; Khaselev, O.; Ramakrishnan, P. A.; Faiman, D.; Katz, E. A.; Shames, A.; Goren, S. *Sol. Energy Mater.* **1998**, *51*, 9.  
(4) (a) Rajpure, K. Y.; Bhosale, C. H. *Mater. Chem. Phys.* **2000**, *63*, 263. (b) Owens, B. B.; Bottelberghe, J. R. *Solid State Ionics* **1993**, *62*, 243. (c) Rajpure, K. Y.; Bhosale, C. H. *Mater. Chem. Phys.* **2000**, *64*, 70.  
(5) (a) Li, B.; Wang, L. D.; Kang, B. N.; Wang, P.; Qiu, Y. *Sol. Energy Mater.* **2006**, *90*, 549. (b) Gratzel, M. *Curr. Opin. Colloid Interface Sci.* **1999**, *4*, 314.  
(6) (a) Link, C.; Pantenburg, I.; Meyer, G. Z. *Anorg. Allg. Chem.* **2008**, *634*, 616. (b) Pantenburg, I.; Muller, I. Z. *Anorg. Allg. Chem.* **2004**, *630*, 1637. (c) Aragoni, M. C.; Arca, M.; Demartin, F.; Devillanova, F. A.; Garau, A.; Isaia, F.; Lippolis, V.; Rizzato, S.; Verani, G. *Inorg. Chim. Acta* **2004**, *357*, 3803.  
(7) Svensson, P. H.; Gorlov, M.; Kloo, L. *Inorg. Chem.* **2008**, *47*, 11464.  
(8) Walbaum, C.; Pantenburg, I.; Junk, P.; Deacon, G. B.; Meyer, G. Z. *Anorg. Allg. Chem.* **2010**, *636*, 1444.  
(9) Tebbe, K. F.; Buchem, R. *Angew. Chem., Int. Ed.* **1997**, *36*, 1345.  
(10) Deplano, P.; Ferraro, J. R.; Mercuri, M. L.; Trogu, E. F. *Coord. Chem. Rev.* **1999**, *188*, 71.  
(11) Calabrese, V. T.; Khan, A. J. *Phys. Chem. A* **2000**, *104*, 1287.  
(12) Fenn, J. B.; Mann, M.; Meng, C. K.; Wong, S. F.; Whitehouse, C. M. *Science* **1989**, *246*, 64.  
(13) Henderson, W.; McIndoe, J. S. *Mass Spectrometry of Inorganic and Organometallic Compounds: Tools, Techniques, Tips*; Wiley: New York, 2005.  
(14) (a) Chisholm, D. M.; Oliver, A. G.; McIndoe, J. S. *Dalton Trans.* **2010**, *39*, 364. (b) McQuinn, K.; Hof, F.; McIndoe, J. S. *Chem. Commun.* **2007**, 4099. (c) Brayshaw, S. K.; Green, J. C.; Hazari, N.; McIndoe, J. S.; Marken, F.; Raithby, P. R.; Weller, A. S. *Angew. Chem., Int. Ed.* **2006**, *45*, 6005.  
(15) Deetlefs, M.; Seddon, K. R.; Shara, M. *Phys. Chem. Chem. Phys.* **2006**, *8*, 642.  
(16) (a) Zistler, M.; Schreiner, C.; Wachter, P.; Wassercheid, P.; Gerhard, D.; Gores, H. J. *Int. J. Electrochem. Sci.* **2008**, *3*, 236. (b) Stegemann, H.; Rohde, A.; Reiche, A.; Schnittke, A.; Fullbier, H. *Electrochim. Acta* **1992**, *37*, 379.  
(17) (a) Dyson, P. J.; McIndoe, J. S.; Zhao, D. *Chem. Commun.* **2003**, 508. (b) Dyson, P. J.; Khalaila, I.; Luetgen, S.; McIndoe, J. S.; Zhao, D. *Chem. Commun.* **2004**, 2204–2205.  
(18) Crawford, E.; McIndoe, J. S.; Tuck, D. G. *Can. J. Chem.* **2006**, *84*, 1607.  
(19) Chen, X. Y.; Rickard, M. A.; Hull, J. W.; Zheng, C.; Leugers, A.; Simoncic, P. *Inorg. Chem.* **2010**, *49*, 8684.  
(20) (a) Sharp, S. B.; Gellene, G. I. J. *Phys. Chem. A* **1997**, *101*, 2192–2197. (b) Ogawa, Y.; Takahashi, O.; Kikuchi, O. *J. Mol. Struct. (Theochem)* **1998**, *424*, 285–292. (c) Calabrese, V. T.; Khan, A. J. *Phys. Chem. A* **2000**, *104*, 1287–1292. (d) Kloo, L.; Rosdahl, J.; Svensson, P. H. *Eur. J. Inorg. Chem.* **2002**, 1203–1209. (e) Asaduzzaman, A. M.; Schreckenbach, G. *Theor. Chem. Acc.* **2009**, *122*, 119–125. (f) Hu, C.-H.; Asaduzzaman, A. M.; Schreckenbach, G. *J. Phys. Chem. C* **2010**, *114*, 15165–15173. (g) Gomes, A. S. P.; Visscher, L.; Bolvin, H.; Saue, T.; Knecht, S.; Fleig, T.; Eliav, E. *J. Chem. Phys.* **2010**, *133*, 064305.  
(21) Tebbe, K.-F.; Dombrowski, I. Z. *Anorg. Allg. Chem.* **1999**, *625*, 167.  
(22) Frisch, M. J.; Trucks, G. W.; Schlegel, H. B.; Scuseria, G. E.; Robb, M. A.; Cheeseman, J. R.; Montgomery, J. A.; Vreven, T.; Kudin, K. N.; Burant, J. C.; Millam, J. M.; Iyengar, S. S.; Tomasi, J.; Barone, V.; Mennucci, B.; Cossi, M.; Scalmani, G.; Rega, N.; Petersson, G. H.; Nakatsuji, H.; Hada, M.; Ehara, M.; Toyota, K.; Fukuda, R.; Hasegawa, J.; Ishida, M.; Nakajima, T.; Honda, Y.; Kitao, O.; Nakai, H.; Klene, M.; Li, X.; Knox, J. E.; Hratchian, H. P.; Cross, J. B.; Adamo, C.; Jaramillo, J.; Gomperts, R.; Stratmann, R. E.; Yazyev, O.; Austin, A. J.; Cammi, R.; Pomelli, C.; Ochterski, J. W.; Ayala, P. Y.; Morokuma, K.; Voth, G. A.; Salvador, P.; Dannenberg, J. J.; Zakrzewski, V. G.; Dapprich, S.; Daniels, A. D.; Strain, M. C.; Farkas, O.; Malick, D. K.; Rabuck, A. D.; Raghavachari, K.; Foresman, J. B.; Ortiz, J. V.; Cui, Q.; Baboul, A. G.;

Clifford, S.; Cioslowski, J.; Stefanov, B. B.; Liu, G.; Liashenko, A.; Piskorz, P.; Komaromi, I.; Martin, R. L.; Fox, D. J.; Keith, T.; M. A. Al-Laham, Peng, C. Y.; Nanayakkara, A.; Challacombe, M.; Gill, P. M. W.; Johnson, B.; Chen, W.; Wong, M. W.; Gonzalez, C.; Pople, J. A. *Gaussian 03*, Revision D.02; Gaussian, Inc.: Wallingford, CT, 2004.

(23) Becke, A. D. *J. Chem. Phys.* **1993**, *98*, 5648–5652.

(24) Lee, C.; Yang, W.; Parr, R. G. *Phys. Rev. B* **1988**, *41*, 785–789.

(25) Peterson, K. A.; Shepler, B. C.; Figgen, D.; Stoll, H. *J. Phys. Chem. A* **2006**, *110*, 13877.

(26) <http://www.theochem.uni-stuttgart.de/pseudopotentials/clickpse.en.html>.